

Augment Density Matrix Renormalization Group with Disentanglers

Xiangjian Qian¹ and Mingpu Qin^{1,*}

¹*Key Laboratory of Artificial Structures and Quantum Control (Ministry of Education),
School of Physics and Astronomy, Shanghai Jiao Tong University, Shanghai 200240, China*

(Dated: June 28, 2022)

Density Matrix Renormalization Group (DMRG) and its extensions in the form of Matrix Product States (MPS) are arguably the choice for the study of one dimensional quantum systems in the last three decades. However, due to the limited entanglement encoded in the wave-function ansatz, to maintain the accuracy of DMRG with the increase of the system size in the study of two dimensional systems, exponentially increased resources are required, which limits the applicability of DMRG to only narrow systems. In this work, we introduce a new ansatz in which DMRG is augmented with disentanglers to encode an entropic area law. In the new method, the $O(D^3)$ low computational cost of DMRG is kept. We perform benchmark calculations with this approach on the two dimensional transverse Ising model and Heisenberg model. Our results show the accuracy is maintained with the increase of the size of two dimensional systems. This new ansatz provides a very useful approach for the study of two-dimensional quantum systems in the future.

PACS numbers:

The study of exotic phases and the phase transitions between them in strongly correlated quantum many-body systems is one of the largest challenges in condensed matter physics [1–3]. The main difficulty stems from the exponential growth of the Hilbert space dimension with the system size, which means brutal force approach can only handle very small systems. Analytic solution to quantum many-body systems is very rare [4–8]. So most studies of these systems rely on different types of numerical methods nowadays [9–17].

Density Matrix Renormalization Group (DMRG) [12–15] is one of the most successful numerical methods for the study of quantum many-body systems in the past decades. DMRG can provide highly accurate result for one dimensional (1D) quantum many-body systems with relative low computational cost [15]. With these advantages, DMRG is now arguably the workhorse for one dimensional systems and many interesting phenomena in one dimension are unveiled with the help of DMRG [18, 19]. But it is known that the physics in two dimension (2D) is richer [20–26] and many exotic states [27–29] exist only in 2D. But the direct application of DMRG to 2D systems (by arranging a 2D system into a 1D one with long-range interactions) is not as successful as the study of 1D cases. It was found that the required resource needs to increase exponentially with the system size in 2D if we want to maintain the accuracy [30], which limits the study of 2D systems with DMRG to narrow ladder or cylindrical systems [31].

It was realized later that the wave-functions obtained by DMRG are actually Matrix Product States (MPS) [32]. In the language of MPS, the success of DMRG lies in the fact that the entanglement encoded in the wave-function satisfy the entropic area law [33–36] of

1D quantum systems. But MPS fails to capture the entropic area law for 2D systems which has to be remedied by exponentially large bond dimensions. To overcome this difficulty, MPS was generalized to high dimension in the perspective of Tensor Network States (TNS) [37, 38]. In TNS, the wave-function of a quantum many-body system is represented as the contraction of connected tensors with polynomial parameters in contrast to the exponentially large Hilbert space. Different types of TNS were proposed in the past, like Projected Entangled Pair States (PEPS) [17, 39–43], Tree Tensor Network (TTN) [44–47], Multiscale Entanglement Renormalization ansatz (MERA) [48–51], and projected entangled simplex states (PESS) [52]. It can be easily proven that 2D PEPS, MERA, and PESS can capture the entropic area law for 2D quantum systems [36, 52, 53] which makes them better wave-function ansatz for 2D systems. Progress in the understanding of exotic physics in 2D has been made with these TNS-related methods in the past [39, 54–58], but the high computational complexity hampers the wide application of them in the study of 2D systems. The typical cost of PEPS is $O(D^{10})$ [59] (We notice that many attempts have been made to low the computation cost of PEPS [39, 60–62]) and $O(D^{16})$ [50] for MERA, which makes calculation with large bond dimension infeasible and limit the power of these methods. So for practical reason, because DMRG and MPS-based approaches are easy to be optimized and the computational cost is low, they are still widely used in the study of 2D (ladder or cylindrical) systems [63–68] by pushing the bond dimension to very large numbers, even though they can't capture the entropic area law for 2D systems intrinsically.

In this work, we introduce a new MPS or DMRG based ansatz dubbed as Fully-Augmented Matrix Product State (FAMPS) by generalizing the idea from augmented-TTN [44, 45] to MPS. In FAMPS, MPS is augmented with disentanglers to increase the entanglement encoded

*qinmingpu@sjtu.edu.cn

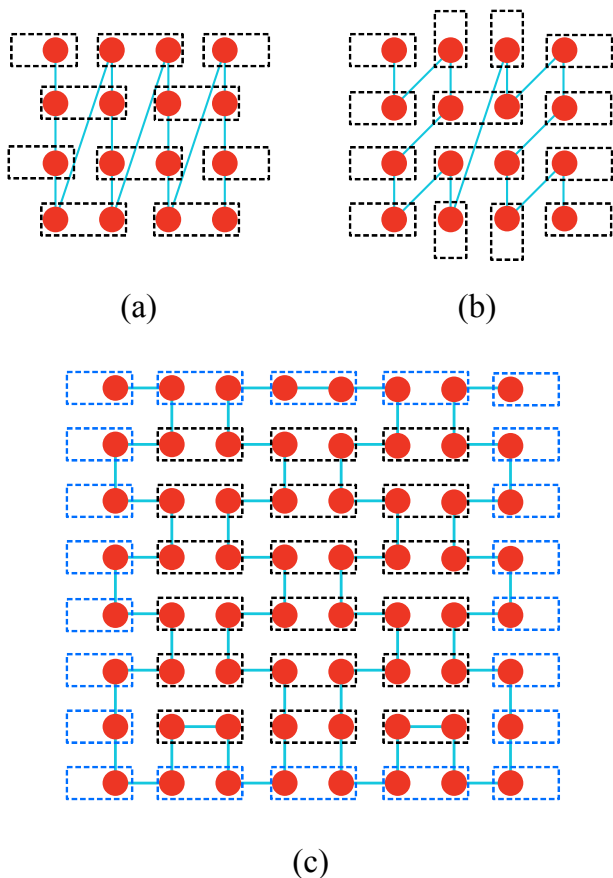


FIG. 1: Different schemes to arrange a 2D lattice into a 1D one in DMRG for periodic boundary conditions. The disentanglers in corresponding FAMPS are denoted as dashed rectangles. (a) The commonly adopted scheme for a 4×4 lattice. (b) A tree-type scheme for a 4×4 lattice (more details can be found in [45]) (c) A new scheme for a 8×8 lattice which is used in this work. When augmented with disentanglers, the FAMPS encodes more entanglement in (b) and (c) than that in (a). The disentanglers at the edges denoted as dashed blue rectangles need to be rearranged for different boundary conditions.

in the wave-function. In the simplest scheme, where disentanglers are placed directly in the physical layer and span only two sites, it can be proved that the entanglement entropy captured in FAMPS scales as $l \ln(d^2)$ with l the measure of the cut with which the system is divided into two parts and d is the dimension of local Hilbert space. Most importantly, the low, i.e., $O(D^3)$ computational cost in DMRG is maintained in FAMPS. Our benchmark results of 2D periodic Heisenberg model show that the accuracy of ground state energy is maintained with the increase of system size with a fixed bond dimension in FAMPS, in contrast to DMRG in which the accuracy is decreased with the increase of system size.

Fully-Augmented Matrix Product States – An MPS is

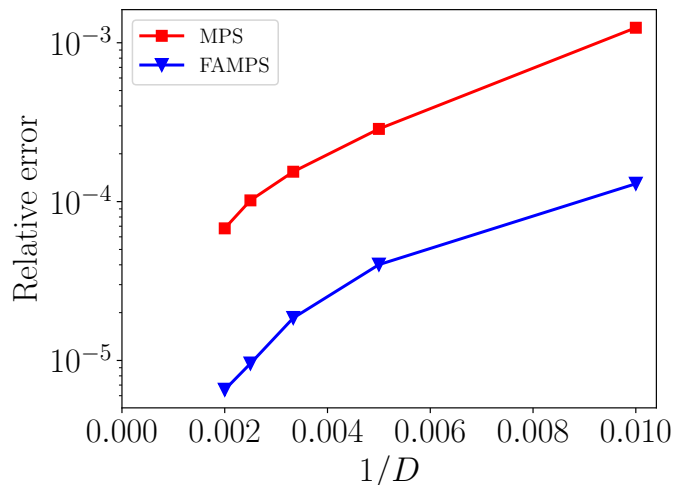


FIG. 2: Relative error of the ground state energy for FAMPS and MPS of the transverse Ising model near the critical point ($\lambda = 3.05$) for a 8×8 lattice with periodic boundary conditions. The scheme in Fig. 1 (c) is used. The reference energy is the extrapolated value of FAMPS results with different bond dimensions (details can be found in the supplementary results). We can find that the improvement of FAMPS over MPS is about one order of magnitude.

defined as

$$|\psi\rangle = \sum_{\{\sigma_i\}} \text{Tr}[A^{\sigma_1} A^{\sigma_2} A^{\sigma_3} \dots A^{\sigma_n}] |\sigma_1 \sigma_2 \sigma_3 \dots \sigma_n\rangle \quad (1)$$

where A is a rank-3 tensor with one physical index σ_i (with dimension d) and two auxiliary indices (with dimension D). It can be easily shown that MPS can capture the entropic area law for 1D system [69, 70], which is the reason behind the success of DMRG. But it fails to capture the entropic area law for 2D system. For this reason, the bond-dimension needs to increase exponentially with system size to achieve a fixed accuracy when studying 2D systems with DMRG.

Disentanglers are common building blocks in TNS which can reduce the local entanglement in the studied system [49]. Following the strategy in [44, 45], we can place an additional disentangler layer on the physical layer of MPS to increase the entanglement in the wave-function as $|\text{FAMPS}\rangle = D(\mu)|\text{MPS}\rangle$, where $D(\mu)$ denotes the disentangler layer.

As discussed in Ref. [45], there are two criterias when placing disentanglers. The first one is that there should be no two disentanglers sharing the same physical site. The other one is to place more disentanglers in places where the maximum entanglement entropy the ansatz wave-function can host is small if the system is divided into two parts. The first criteria ensures a comparable computational complexity with its predecessor (with a factor of d^4 at the worst case). The second criteria is to make the entanglement distribute as uniform as possible in the whole system in order to ensure the least

entanglement in the wave-function for different cuts as large as possible, because the number of disentanglers is constrained by the first criteria.

The special structure of FAMPS suggests that the optimization process of FAMPS can be divided into two steps. First, the disentanglers can be optimized using the standard Evenbly-Vidal algorithm [71]. Second, the rest tensors can be directly optimized with the traditional MPS or DMRG optimization procedure. More details can be found in the supplementary materials.

The arrangement of a 2D lattice to a 1D one in DMRG was extensively studied in the past [47, 72]. In the DMRG calculation, different arrangements have small effect on the accuracy as will be shown late. However, the way a 2D lattice is arranged in a 1D one is crucial when augmenting MPS with disentanglers, which determines the amount of entanglement the wave-function can encode. In Fig. 1, we show three different ways to arrange the 2D lattice in a 1D one. The scheme in Fig. 1 (a) is the most common used one in the literature. In this scheme, the entanglement is large if we cut the system horizontally, while only one bond is crossed if the system is cut vertically. This means an MPS in the scheme of Fig. 1 (a) can only encode an entanglement entropy $S \leq \ln(D)$. Then in order to capture the entropic area law for 2D systems, the bond dimension need to scale exponentially with system width as $D = e^{cL}$, where c is a constant and L is the width of the system. To augment MPS with disentanglers based on the scheme in Fig. 1 (a), we need to place all the disentanglers (the dashed rectangulars in Fig. 1 (a)) horizontally according the two criterias mentioned above. Because we can only place $L/2$ disentanglers horizontally in each column and the entanglement entropy contributed by each disentangler is maximally $\ln(d^2)$, the maximum entanglement entropy the FAMPS in Fig. 1 (a) can encode satisfies an area law as $L \ln(d)$.

We have more efficient way to place the disentanglers. In Fig. 1 (c), we introduce another scheme to arrange the 2D lattice in a 1D one. The entanglement in the MPS in Fig. 1 (c) is more uniformly distributed than that in Fig. 1 (a) [73]. When augmented with disentanglers, the maximum entanglement entropy encoded in the FAMPS in Fig. 1 (c) is $L \ln(d^2)$ which is twice that in Fig. 1 (a). Comparing to Fig. 1 (a), the number of crossed bonds with horizontal cut is reduced by a half, but even a small $D = d^4$ can support the $L \ln(d^2)$ entanglement entropy for these cuts. Actually Fig. 1 (c) is not the only scheme to support the $L \ln(d^2)$ entanglement entropy, another example is shown Fig. 1 (b), which is analyzed in Ref. [45] based on TTN. In this work, we mainly focus on the scheme in Fig. 1 (c).

Results on the transverse Ising model – We first test FAMPS in the two dimensional transverse Ising model. The Hamiltonian of transverse Ising model is

$$H_{\text{Ising}} = - \sum_{\langle i,j \rangle} \sigma_i^z \sigma_j^z - \lambda \sum_i \sigma_i^x \quad (2)$$

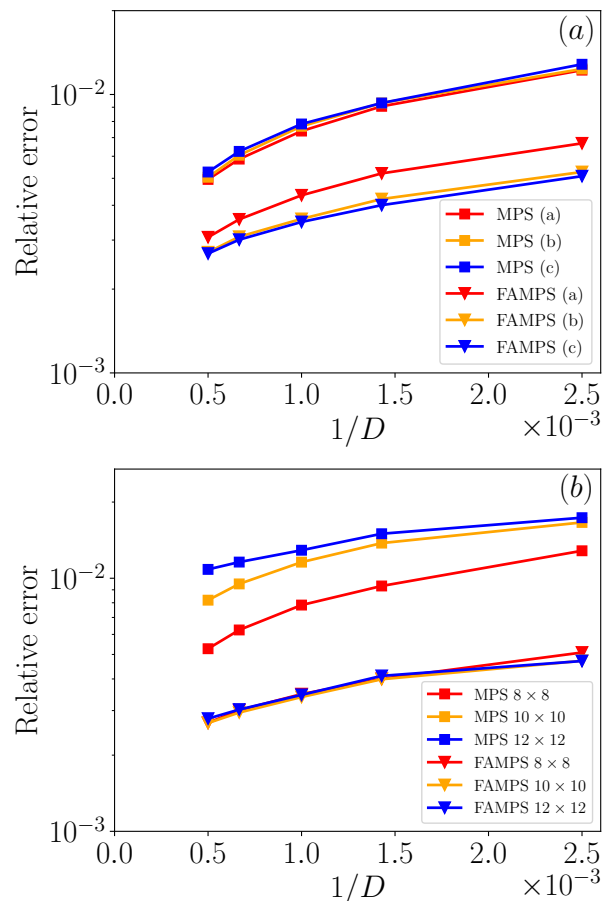


FIG. 3: Relative error of the ground state energy for FAMPS and MPS of the Heisenberg model with periodic boundary conditions. The reference energies are the numerically exact Quantum Monte Carlo results [10]. (a) We compare the results of different schemes in Fig. 1. ((a), (b), and (c) in the legend denote the different schemes in Fig. 1 (a), (b), and (c) respectively). We can see that the different schemes have little differences in DMRG energy. But after augmented with disentanglers, the FAMPS in Fig. 1 (c) gives lower energy than that in Fig. 1 (a) as expected. (b) We compare the results of different lattice sizes using the scheme in Fig. 1 (c). We can see that FAMPS accuracy is maintained with the increase of lattice size while MPS accuracy becomes worse as anticipated.

where $\{\sigma_i^x, \sigma_i^z\}$ are Pauli matrices. In Fig. 2, we show the relative error of ground state energy from FAMPS and MPS simulations with transverse field $\lambda = 3.05$ (close to the phase transition point of the model). The system is with size 8×8 and with periodic boundary conditions. We use the extrapolated FAMPS result as the reference energy. The details of extrapolation can be found in the supplementary materials. As shown in Fig. 2, we can find that FAMPS is about one order of magnitude more accurate than MPS, which is similar to the improvement of FATTN over TTN in Ref. [45].

Results on the Heisenberg model – We also test FAMPS

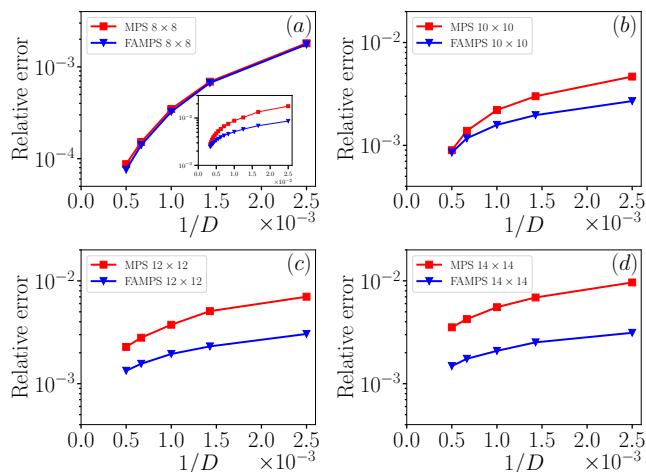


FIG. 4: Relative error of the ground state energy for FAMPS and MPS of the Heisenberg model for lattice sizes 8×8 , 10×10 , 12×12 , and 14×14 with open boundary conditions. The reference energy is the numerically exact results obtained by Quantum Monte Carlo in [39]. When system size is small, the improvement of FAMPS over MPS is not obvious as shown in (a) and (b) and we find that there exists a critical bond dimension after which the energies from FAMPS and MPS are identical. This is mainly due to that MPS is able to capture the entanglement of a small system with a moderate bond-dimension. However, with the increase of system size, the improvement becomes more and more significant.

on the 2D Heisenberg model whose ground state is more entangled than the transverse Ising model. The Hamiltonian of Heisenberg model is

$$H_{\text{Heisenberg}} = \sum_{\langle i,j \rangle} S_i S_j \quad (3)$$

where S_i denote the spin of site i . We consider only nearest neighboring interactions. Here, we take advantage of the $U(1)$ symmetry [74] in our simulation. We take the numerically exact Quantum Monte Carlo results [10, 39] as references. First, we calculate the ground state energy for 8×8 lattice with periodic boundary conditions to test FAMPS with different schemes to arrange the 2D lattice in 1D. Fig. 3 (a) shows the relative error of the ground state energy as a function of bond-dimension. We can find that the energies from MPS without disentangler layer have little differences for the three schemes in Fig. 1. This result agrees with the study in [47, 72] which shows different arrangements can lead to increased numerical precision but not very significant for two-dimension systems. The underlying reason is that no matter how to arrange a 2D lattice in 1D, we can not get rid of the requirement for an exponentially large bond-dimension to capture the entropic area law for 2D systems. However, when augmented with disentanglers, FAMPS results in Fig. 3 (a) show the differences in accuracy is significant for different arrangement schemes. As expected, the FAMPS in Fig. 1 (c) is more accurate than that in Fig. 1 (a) because

the entanglement encoded in the wave-function ansatz in (c) is larger. For the Heisenberg model, the improvement in accuracy is about half an order of magnitude.

We then test FAMPS with larger sizes using the scheme in Fig. 1 (c) which encodes more entanglement and gives more accurate energy. In Fig. 3 (b), we show the relative error of the ground state energy for lattice sizes 8×8 , 10×10 , and 12×12 . The most important finding in these results is that the accuracy of FAMPS is maintained with the increase of lattice size, despite the accuracy of MPS is decreased with the increase of lattice size as expected. As discussed early, MPS can not capture the entropic area law which means the bond dimension needs to increase exponentially to maintain the accuracy. But with the help of disentanglers, FAMPS can capture the entropic area law and can remedy the requirement of exponential growth of bond dimension. This property makes FAMPS a promising method in the study of two dimensional systems in the future.

At last, we test FAMPS for Heisenberg model with open boundary conditions, which is easier to handle than periodic systems. We calculate the ground state energy with system sizes 8×8 , 10×10 , 12×12 , and 14×14 . As shown in the inset of Fig. 4 (a), the improvement of FAMPS over MPS decreases with the increase of bond dimension, and they become identical after a critical bond dimension, which means the optimized disentanglers are just identity operators after the critical bond dimension [75]. Similar results are obtained for cylinder systems. Details can be found in the supplementary materials. By comparing the four panels in Fig. 4, we find that the critical bond dimension where FAMPS and MPS energy becomes identical increases with the system size. For small system with open boundary conditions, a moderate bond dimension D can already capture the entanglement of the ground state. But when the system becomes larger, the entanglement in the ground state increase according to the entropic area law, which means the improvement of energy with disentanglers in FAMPS will increase with the increase of system size for a fixed bond dimension. In this sense, FAMPS is more useful for “hard” problems where large bond dimension is required for MPS.

Conclusions – In this work, we propose a new ansatz, FAMPS, by augmenting MPS with disentanglers. FAMPS can encode the entropic area law for two dimensional quantum systems and at the same time keeps the low $O(D^3)$ computational cost. We carry out benchmark calculations of FAMPS on the 2D transverse Ising model near critical point and 2D Heisenberg model. For the Heisenberg model with periodic boundary conditions, we find that the accuracy is maintained in FAMPS with the increase of system size while in MPS the bond dimension needs to increase exponentially to achieve that. FAMPS provides a useful approach for the study of 2D problems for which DMRG has difficulty to provide accurate result [63]. FAMPS can be generalized to encode more entanglement by placing multiple layers of disentanglers to MPS. The area law encoded in FAMPS can also benefit

many other MPS based approaches, e.g., the simulation of time evolution or the dynamic properties [76–78].

Acknowledgments

The calculation in this work is carried out with Quimb [79].

-
- [1] D. Cabra, A. Honecker, and P. Pujol, *Modern Theories of Many-Particle Systems in Condensed Matter Physics*, vol. 843 (2012), ISBN 978-3-642-10448-0.
- [2] X. G. Wen, *Quantum field theory of many-body systems: from the origin of sound to an origin of light and electrons* (Oxford University Press, Oxford, 2007), URL <https://cds.cern.ch/record/803748>.
- [3] E. C. Marino, *Quantum Field Theory Approach to Condensed Matter Physics* (Cambridge University Press, Cambridge, 2017).
- [4] A. J. Berlinsky and A. B. Harris, *The Ising Model: Exact Solutions* (Springer International Publishing, Cham, 2019), pp. 441–476, ISBN 978-3-030-28187-8, URL https://doi.org/10.1007/978-3-030-28187-8_17.
- [5] J. Dukelsky, S. Pittel, and G. Sierra, *Rev. Mod. Phys.* **76**, 643 (2004), URL <https://link.aps.org/doi/10.1103/RevModPhys.76.643>.
- [6] E. H. Lieb and F. Y. Wu, *Phys. Rev. Lett.* **20**, 1445 (1968), URL <https://link.aps.org/doi/10.1103/PhysRevLett.20.1445>.
- [7] Y. Qiao, P. Sun, Z. Xin, J. Cao, and W.-L. Yang, *Journal of Physics A: Mathematical and Theoretical* **53**, 075205 (2020), URL <https://doi.org/10.1088/1751-8121/ab6a32>.
- [8] H. Zou, E. Zhao, X.-W. Guan, and W. V. Liu, *Phys. Rev. Lett.* **122**, 180401 (2019), URL <https://link.aps.org/doi/10.1103/PhysRevLett.122.180401>.
- [9] J. E. Hirsch, R. L. Sugar, D. J. Scalapino, and R. Blankenbecler, *Phys. Rev. B* **26**, 5033 (1982), URL <https://link.aps.org/doi/10.1103/PhysRevB.26.5033>.
- [10] A. W. Sandvik, *Phys. Rev. B* **56**, 11678 (1997), URL <https://link.aps.org/doi/10.1103/PhysRevB.56.11678>.
- [11] W. J. Huggins, B. A. O’Gorman, N. C. Rubin, D. R. Reichman, R. Babbush, and J. Lee, *Nature* **603**, 416 (2022), ISSN 1476-4687, URL <https://doi.org/10.1038/s41586-021-04351-z>.
- [12] S. R. White, *Phys. Rev. Lett.* **69**, 2863 (1992), URL <https://link.aps.org/doi/10.1103/PhysRevLett.69.2863>.
- [13] S. R. White, *Phys. Rev. B* **48**, 10345 (1993), URL <https://link.aps.org/doi/10.1103/PhysRevB.48.10345>.
- [14] U. Schollwöck, *Rev. Mod. Phys.* **77**, 259 (2005), URL <https://link.aps.org/doi/10.1103/RevModPhys.77.259>.
- [15] U. Schollwöck, *Annals of Physics* **326**, 96 (2011), ISSN 0003-4916, january 2011 Special Issue, URL <https://www.sciencedirect.com/science/article/pii/S0003491610001752>.
- [16] J. P. F. LeBlanc, A. E. Antipov, F. Becca, I. W. Bulik, G. K.-L. Chan, C.-M. Chung, Y. Deng, M. Ferrero, T. M. Henderson, C. A. Jiménez-Hoyos, et al. (Simons Collaboration on the Many-Electron Problem), *Phys. Rev. X* **5**, 041041 (2015), URL <https://link.aps.org/doi/10.1103/PhysRevX.5.041041>.
- [17] J. I. Cirac, D. Pérez-García, N. Schuch, and F. Verstraete, *Rev. Mod. Phys.* **93**, 045003 (2021), URL <https://link.aps.org/doi/10.1103/RevModPhys.93.045003>.
- [18] E. M. Stoudenmire, L. O. Wagner, S. R. White, and K. Burke, *Phys. Rev. Lett.* **109**, 056402 (2012), URL <https://link.aps.org/doi/10.1103/PhysRevLett.109.056402>.
- [19] K. Hida, *Phys. Rev. Lett.* **83**, 3297 (1999), URL <https://link.aps.org/doi/10.1103/PhysRevLett.83.3297>.
- [20] H. Nakano, Y. Minami, and S.-i. Sasa, *Phys. Rev. Lett.* **126**, 160604 (2021), URL <https://link.aps.org/doi/10.1103/PhysRevLett.126.160604>.
- [21] I. A. Verzhbitskiy, D. Voiry, M. Chhowalla, and G. Eda, *2D Materials* **7**, 035013 (2020), URL <https://doi.org/10.1088/2053-1583/ab8690>.
- [22] G. E. Astrakharchik, I. L. Kurbakov, D. V. Sychev, A. K. Fedorov, and Y. E. Lozovik, *Phys. Rev. B* **103**, L140101 (2021), URL <https://link.aps.org/doi/10.1103/PhysRevB.103.L140101>.
- [23] B. Dalla Piazza, M. Mourigal, N. B. Christensen, G. J. Nilsen, P. Tregenna-Piggott, T. G. Perring, M. Enderle, D. F. McMorrow, D. A. Ivanov, and H. M. Rønnow, *Nature Physics* **11**, 62 (2015), ISSN 1745-2481, URL <https://doi.org/10.1038/nphys3172>.
- [24] A. W. W. Ludwig, D. Poilblanc, S. Trebst, and M. Troyer, *New Journal of Physics* **13**, 045014 (2011), URL <https://doi.org/10.1088/1367-2630/13/4/045014>.
- [25] M. Brooks, M. Leshko, D. Lundholm, and E. Yakaboylu, *Phys. Rev. Lett.* **126**, 015301 (2021), URL <https://link.aps.org/doi/10.1103/PhysRevLett.126.015301>.
- [26] C. Han, Z. Iftikhar, Y. Kleeorin, A. Anthore, F. Pierre, Y. Meir, A. K. Mitchell, and E. Sela, *Phys. Rev. Lett.* **128**, 146803 (2022), URL <https://link.aps.org/doi/10.1103/PhysRevLett.128.146803>.
- [27] D. Arovas, J. R. Schrieffer, and F. Wilczek, *Phys. Rev. Lett.* **53**, 722 (1984), URL <https://link.aps.org/doi/10.1103/PhysRevLett.53.722>.
- [28] B. I. Halperin, *Phys. Rev. Lett.* **52**, 1583 (1984), URL <https://link.aps.org/doi/10.1103/PhysRevLett.52.1583>.
- [29] F. Wilczek, *Phys. Rev. Lett.* **49**, 957 (1982), URL <https://link.aps.org/doi/10.1103/PhysRevLett.49.957>.
- [30] S. Liang and H. Pang, *Phys. Rev. B* **49**, 9214 (1994), URL <https://link.aps.org/doi/10.1103/PhysRevB.49.9214>.

- 49.9214.
- [31] E. Stoudenmire and S. R. White, Annual Review of Condensed Matter Physics **3**, 111 (2012), <https://doi.org/10.1146/annurev-conmatphys-020911-125018>, URL <https://doi.org/10.1146/annurev-conmatphys-020911-125018>.
- [32] S. Östlund and S. Rommer, Phys. Rev. Lett. **75**, 3537 (1995), URL <https://link.aps.org/doi/10.1103/PhysRevLett.75.3537>.
- [33] M. B. Plenio, J. Eisert, J. Dreißig, and M. Cramer, Phys. Rev. Lett. **94**, 060503 (2005), URL <https://link.aps.org/doi/10.1103/PhysRevLett.94.060503>.
- [34] G. Vidal, J. I. Latorre, E. Rico, and A. Kitaev, Phys. Rev. Lett. **90**, 227902 (2003), URL <https://link.aps.org/doi/10.1103/PhysRevLett.90.227902>.
- [35] M. Srednicki, Phys. Rev. Lett. **71**, 666 (1993), URL <https://link.aps.org/doi/10.1103/PhysRevLett.71.666>.
- [36] J. Eisert, M. Cramer, and M. B. Plenio, Rev. Mod. Phys. **82**, 277 (2010), URL <https://link.aps.org/doi/10.1103/RevModPhys.82.277>.
- [37] R. Orús, Nature Reviews Physics **1**, 538 (2019), ISSN 2522-5820, URL <https://doi.org/10.1038/s42254-019-0086-7>.
- [38] J. C. Bridgeman and C. T. Chubb, Journal of Physics A: Mathematical and Theoretical **50**, 223001 (2017), URL <https://doi.org/10.1088/1751-8121/aa6dc3>.
- [39] W.-Y. Liu, Y.-Z. Huang, S.-S. Gong, and Z.-C. Gu, Phys. Rev. B **103**, 235155 (2021), URL <https://link.aps.org/doi/10.1103/PhysRevB.103.235155>.
- [40] G. Scarpa, A. Molnár, Y. Ge, J. J. García-Ripoll, N. Schuch, D. Pérez-García, and S. Iblisdir, Phys. Rev. Lett. **125**, 210504 (2020), URL <https://link.aps.org/doi/10.1103/PhysRevLett.125.210504>.
- [41] H.-J. Liao, J.-G. Liu, L. Wang, and T. Xiang, Phys. Rev. X **9**, 031041 (2019), URL <https://link.aps.org/doi/10.1103/PhysRevX.9.031041>.
- [42] C. Hubig, SciPost Phys. **5**, 47 (2018), URL <https://scipost.org/10.21468/SciPostPhys.5.5.047>.
- [43] L. Vanderstraeten, L. Burgelman, B. Ponsioen, M. Van Damme, B. Vanhecke, P. Corboz, J. Haegeman, and F. Verstraete, Phys. Rev. B **105**, 195140 (2022), URL <https://link.aps.org/doi/10.1103/PhysRevB.105.195140>.
- [44] T. Felser, S. Notarnicola, and S. Montangero, Phys. Rev. Lett. **126**, 170603 (2021), URL <https://link.aps.org/doi/10.1103/PhysRevLett.126.170603>.
- [45] X. Qian and M. Qin, Phys. Rev. B **105**, 205102 (2022), URL <https://link.aps.org/doi/10.1103/PhysRevB.105.205102>.
- [46] P. Silvi, F. Tschirsich, M. Gerster, J. Jünemann, D. Jaschke, M. Rizzi, and S. Montangero, SciPost Phys. Lect. Notes p. 8 (2019), URL <https://scipost.org/10.21468/SciPostPhysLectNotes.8>.
- [47] G. Cataldi, A. Abedi, G. Magnifico, S. Notarnicola, N. D. Pozza, V. Giovannetti, and S. Montangero, Quantum **5**, 556 (2021), ISSN 2521-327X, URL <https://doi.org/10.22331/q-2021-09-29-556>.
- [48] J. C. Bridgeman, A. O'Brien, S. D. Bartlett, and A. C. Doherty, Phys. Rev. B **91**, 165129 (2015), URL <https://link.aps.org/doi/10.1103/PhysRevB.91.165129>.
- [49] G. Vidal, Phys. Rev. Lett. **101**, 110501 (2008), URL <https://link.aps.org/doi/10.1103/PhysRevLett.101.110501>.
- [50] G. Evenbly and G. Vidal, Phys. Rev. Lett. **102**, 180406 (2009), URL <https://link.aps.org/doi/10.1103/PhysRevLett.102.180406>.
- [51] G. Vidal, Phys. Rev. Lett. **99**, 220405 (2007), URL <https://link.aps.org/doi/10.1103/PhysRevLett.99.220405>.
- [52] Z. Y. Xie, J. Chen, J. F. Yu, X. Kong, B. Normand, and T. Xiang, Phys. Rev. X **4**, 011025 (2014), URL <https://link.aps.org/doi/10.1103/PhysRevX.4.011025>.
- [53] F. Verstraete, M. M. Wolf, D. Perez-Garcia, and J. I. Cirac, Phys. Rev. Lett. **96**, 220601 (2006), URL <https://link.aps.org/doi/10.1103/PhysRevLett.96.220601>.
- [54] G. Evenbly and G. Vidal, Phys. Rev. Lett. **104**, 187203 (2010), URL <https://link.aps.org/doi/10.1103/PhysRevLett.104.187203>.
- [55] P. Corboz and F. Mila, Phys. Rev. Lett. **112**, 147203 (2014), URL <https://link.aps.org/doi/10.1103/PhysRevLett.112.147203>.
- [56] H. J. Liao, Z. Y. Xie, J. Chen, Z. Y. Liu, H. D. Xie, R. Z. Huang, B. Normand, and T. Xiang, Phys. Rev. Lett. **118**, 137202 (2017), URL <https://link.aps.org/doi/10.1103/PhysRevLett.118.137202>.
- [57] B.-X. Zheng, C.-M. Chung, P. Corboz, G. Ehlers, M.-P. Qin, R. M. Noack, H. Shi, S. R. White, S. Zhang, and G. K.-L. Chan, Science **358**, 1155 (2017), ISSN 0036-8075, 1095-9203, URL <http://science.sciencemag.org/content/358/6367/1155>.
- [58] W.-Y. Liu, S.-S. Gong, Y.-B. Li, D. Poilblanc, W.-Q. Chen, and Z.-C. Gu, Science Bulletin **67**, 1034 (2022), ISSN 2095-9273, URL <https://www.sciencedirect.com/science/article/pii/S2095927322001001>.
- [59] M. Lubasch, J. I. Cirac, and M.-C. Bañuls, Phys. Rev. B **90**, 064425 (2014), URL <https://link.aps.org/doi/10.1103/PhysRevB.90.064425>.
- [60] Z. Y. Xie, H. J. Liao, R. Z. Huang, H. D. Xie, J. Chen, Z. Y. Liu, and T. Xiang, Phys. Rev. B **96**, 045128 (2017), URL <https://link.aps.org/doi/10.1103/PhysRevB.96.045128>.
- [61] M. T. Fishman, L. Vanderstraeten, V. Zauner-Stauber, J. Haegeman, and F. Verstraete, Phys. Rev. B **98**, 235148 (2018), URL <https://link.aps.org/doi/10.1103/PhysRevB.98.235148>.
- [62] M. Qin, Phys. Rev. B **102**, 125143 (2020), URL <https://link.aps.org/doi/10.1103/PhysRevB.102.125143>.
- [63] S.-S. Gong, W. Zhu, D. N. Sheng, O. I. Motrunich, and M. P. A. Fisher, Phys. Rev. Lett. **113**, 027201 (2014), URL <https://link.aps.org/doi/10.1103/PhysRevLett.113.027201>.
- [64] S. Yan, D. A. Huse, and S. R. White, Science **332**, 1173 (2011), <https://www.science.org/doi/pdf/10.1126/science.1201080>, URL <https://www.science.org/doi/abs/10.1126/science.1201080>.
- [65] M. Qin, C.-M. Chung, H. Shi, E. Vitali, C. Hubig, U. Schollwöck, S. R. White, and S. Zhang (Simons Collaboration on the Many-Electron Problem), Phys. Rev. X **10**, 031016 (2020), URL <https://link.aps.org/doi/10.1103/PhysRevX.10.031016>.
- [66] H.-C. Jiang and S. A. Kivelson, Phys. Rev. Lett. **127**, 097002 (2021), URL <https://link.aps.org/doi/10.1103/PhysRevLett.127.097002>.
- [67] S. Gong, W. Zhu, and D. N. Sheng, Phys. Rev. Lett. **127**, 097003 (2021), URL <https://link.aps.org/doi/10.1103/PhysRevLett.127.097003>.

- 10.1103/PhysRevLett.127.097003.
- [68] S. Jiang, D. J. Scalapino, and S. R. White, Proceedings of the National Academy of Sciences **118**, e2109978118 (2021), <https://www.pnas.org/doi/pdf/10.1073/pnas.2109978118>, URL <https://www.pnas.org/doi/abs/10.1073/pnas.2109978118>.
- [69] M. B. Hastings, Journal of Statistical Mechanics: Theory and Experiment **2007**, P08024 (2007), URL <https://doi.org/10.1088/1742-5468/2007/08/p08024>.
- [70] T. Kuwahara and K. Saito, Nature Communications **11**, 4478 (2020), ISSN 2041-1723, URL <https://doi.org/10.1038/s41467-020-18055-x>.
- [71] G. Evenbly and G. Vidal, Phys. Rev. B **79**, 144108 (2009), URL <https://link.aps.org/doi/10.1103/PhysRevB.79.144108>.
- [72] T. Xiang, J. Lou, and Z. Su, Phys. Rev. B **64**, 104414 (2001), URL <https://link.aps.org/doi/10.1103/PhysRevB.64.104414>.
- [73] We can still easily find vertical cut which crosses only one bond, but the number of these cuts is smaller.
- [74] S. Singh, R. N. C. Pfeifer, and G. Vidal, Phys. Rev. B **83**, 115125 (2011), URL <https://link.aps.org/doi/10.1103/PhysRevB.83.115125>.
- [75] In the actual calculation, we indeed find the disentangles turn to identity operators after the critical bond dimension.
- [76] S. Paeckel, T. Köhler, A. Swoboda, S. R. Manmana, U. Schollwöck, and C. Hubig, Annals of Physics **411**, 167998 (2019), ISSN 0003-4916, URL <https://www.sciencedirect.com/science/article/pii/S0003491619302532>.
- [77] M. C. Bañuls, M. B. Hastings, F. Verstraete, and J. I. Cirac, Phys. Rev. Lett. **102**, 240603 (2009), URL <https://link.aps.org/doi/10.1103/PhysRevLett.102.240603>.
- [78] S. R. White and A. E. Feiguin, Phys. Rev. Lett. **93**, 076401 (2004), URL <https://link.aps.org/doi/10.1103/PhysRevLett.93.076401>.
- [79] J. Gray, Journal of Open Source Software **3**, 819 (2018).

Appendix A: SUPPLEMENTARY MATERIAL

1. More results

In Fig. 5, we show the extrapolation of FAMPS energy with bond dimension for the transverse Ising model with periodic boundary conditions and $\lambda = 3.05$ on a 8×8 lattice. A quadratic fit gives the extrapolated value of ground state energy per site $E = -3.24165(1)$, which is used as reference value in the main text.

In Fig. 6, we show the relative error of energies from FAMPS and MPS for a cylinder system with size 8×8 . Similar as the OBC result in the main text, there exist a critical bond dimension (about $D = 300$, close to the OBC value) after which the two results are the same.

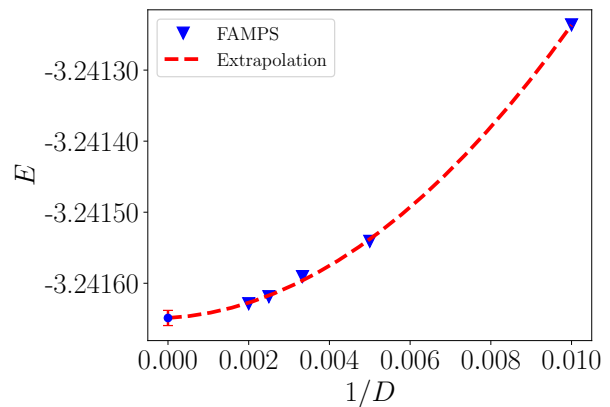


FIG. 5: A quadratic extrapolation of the ground state energy per site of a 8×8 transverse Ising model with $\lambda = 3.05$ from FAMPS.

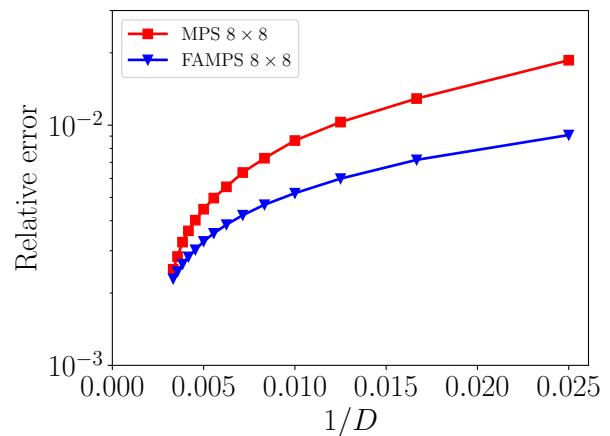


FIG. 6: Relative error of the ground state energy from FAMPS and MPS of the Heisenberg model on a 8×8 lattice with cylinder boundary conditions. Here, we compare our results with the result calculated by MPS with bond-dimension $D = 2500$ which gives an energy of -0.64607 per site.

2. Augmenting MPS with four-site disentangles

We also test an ansatz with disentangles spanning four physical sites (FAMPS4), which encodes more entanglement in the wave-function. The comparison of energies from MPS, FAMPS and FAMPS4 are shown in Fig. 7. We can see an obvious improvement of accuracy of FAMPS4 over FAMPS. We need to mention that the cost of FAMPS4 is $O(D^3 d^8)$ which is higher than FAMPS.

3. Optimization of FAMPS

The optimization process of FAMPS is divided into two steps: the optimization of disentangles and the optimization of the regular MPS tensors. For the optimiza-

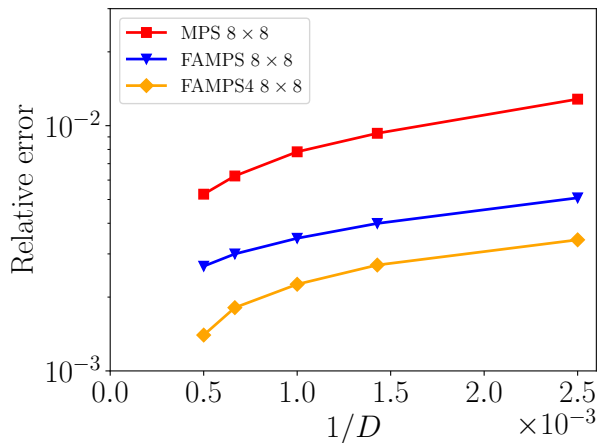


FIG. 7: Relative error of the ground state energy from FAMPS, MPS, and FAMPS4 of the 8×8 Heisenberg model with periodic boundary conditions. The FMPS4 gives the best result as expected.

tion of disentanglers, we follow the procedure shown in Ref. [44, 71]

- (i) select a disentangler μ , calculate the environment E for this disentangler.
- (ii) perform a Singular Value Decomposition (SVD) for environment $E = USV^\dagger$, then calculate the optimized disentangler $\mu_{\text{new}} = -VU^\dagger$.
- (iii) move to another disentangler and iterate procedure (i) and (ii) until all the disentanglers are optimized once.

For the optimization of regular MPS tensors, we first calculate the effective Hamiltonian using the optimized disentanglers $H_{\text{eff}} = D^\dagger(\mu)HD(\mu)$, then use a single site optimization with subspace expansion to optimize MPS tensors based on H_{eff} . The eigenvalue and eigenvector calculation is based on Lanczos algorithm with a few iteration steps (3 ~ 5). Then, we iterate the process mentioned above until the energy is converged.